

# STABILITY ANALYSIS OF A COAL COMBUSTION RESIDUALS IMPOUNDMENT

**Mihai VERDEȘ** – PhD Student, Technical University of Civil Engineering, Faculty of Hydrotechnics,  
e-mail: mihaiivrd@gmail.com

**Abstract:** The overall stability of the Rovinari dry ash slurry impoundment is analyzed using a coupled seepage-stability analysis with the Finite Element Method in a bidimensional model.

To better understand the behavior of such a complex structure, based on the material properties presented in Table 2, the hypotheses presented in Table 4 and described as such, a number of 9 general hypotheses were analyzed, at 178.00 m a.s.l. deposit elevation and final designed height of approximately 35.30 m which corresponds to 191.3 m a.s.l.. The results are presented in tabular form, only 8 diagrams are selected which show the Factor of Safety for hypothesis 0 and 3 which are considered to best describe the real-life conditions regarding the boundary conditions used.

The results show that even at maximum designed height, the deposit is stable in the most realistic worst-case hypothesis 3, with a Factor of Safety of 1.177.

**Keywords:** Finite Element Method, Dry Ash Storage, Embankment Dam, Factor of Safety

## 1. Introduction

### 1.1 General description

Oltenia Energetic Complex is a state-owned company that activates in the production and distribution of electrical energy sector. The electrical energy is produced in coal-fired power plants as a result of burning lignite coal. The process involves multiple stages in which the heat obtained from the burning process is converted into steam that powers a turbine/s which in turn, powers an electric generator.

The end result of this process is electrical energy and as a residual, the fly ash and slag of the burned coal also known as CCRs, coal combustion residuals. This residual must be disposed of, subject of many studies, regarding different methods of reusing, recycling or depositing the CCRs.

This paper addresses the practice of depositing the CCRs, creating what is called a Dry Ash Pond, with respect to the stability of the ash deposit. The case study in this regard is the ash and slag impoundment Gârla created by the deposited CCRs from the Rovinari coal-fired power plant.

### 1.2 Location

The coal-fired power plant Rovinari is located in Rovinari, a town in Gorj County, Romania. The Dry Ash Pond Gârla used by the power plant to deposit the resulting CCRs is located near the power plant at approximately 4,50 km NN-E direction, upstream of the plant, on the left bank of Jiu river, see Fig. 1.



Fig. 1 - Location of Gârla Dry Ash Pond

## 2. Dry Ash Pond Technology

One method of disposal regarding the resulting CCRs produced at a coal-fired power plant is to store the ash in Ash Ponds or impoundments, wet or dry. These deposits have a crucial role in the production of energy, without them a coal-fired power plant cannot function as the resulting volume of CCRs is significant and any other option of disposal is immediately disconsidered because of high costs involved and environmental regulations.

The Rovinari power plant can produce at maximum capacity approximately  $3 \times 10^6 m^3$  of ash and slag per year. This large quantity of material has to be stored in a safe and regulated method.

The Gârla Dry Ash Pond occupies a surface equal to approximately  $1.6 \times 10^6 m^2$  and is designed to have 3 storage compartments (only 2 compartments in present day, see Fig. 2) for storing CCRs over a lifespan of 15 years, in which a total designed capacity of approximately  $32 \times 10^6 m^3$  of CCRs will be stored.



Fig. 2 - Gârla Dry Ash Pond Satellite View

To create the impoundment needed to store the large quantities of ash, a perimetral embankment dam was constructed on the V-S-E sides of the deposit, the N side impoundment is realized by the slope created from the overburden and tailings that results from the coal extraction process.

The base dam or perimetral dam has a variable height ranging from 2.50 m to 10.50 m, made from the local overburden (clay), a crest width of approximately 5.00 m, the general slopes are 1:3, and is equipped with a base drain at the interior toe of the dam, inside the deposit and relief drains in the body of the dam.

The ash is transported from the power plant to the Ash Pond by hydraulic pumping in pipelines over a distance of approximately 3.50 km. The liquid formed by mixing water with CCRs in a 1:1 – 1:1.3 water:solid ratio is called ash slurry or fly ash slurry.

Once the impoundment is filled with slurry at its maximum capacity a new dike is built on top of the perimetral dam to create a new volume for depositing the ash slurry. This dike is smaller than the base dam and is made from a mixture of overburden and dry ash slurry collected from the deposit, also known as dense slurry. The dikes have a height of 3.60 m with slopes of 1:3 on the exterior of the deposit and 1:2 on the interior side of the deposit. They are also equipped with toe drains inside the deposit. See section in Fig. 3 and Fig.4, chapter 3.

### 3. Modeling methods and properties of materials

#### 3.1 Analyzed section

Compartment 2 of Gârla Impoundment is designed to achieve a maximum height of approximately 35.30 m with respect to ground level which is 155.90 m a.s.l. and the crest of the last dike is at 191.30 m a.s.l..

The compartment currently has a height of approximately 22.00 m that corresponds to 178.00 m a.s.l..

Section A-A, presented in Fig. 3, was selected due to the configuration of the terrain, the perimetral dam in this section has the maximum height of 10.50 m, thus representing a good candidate for the stability analysis.

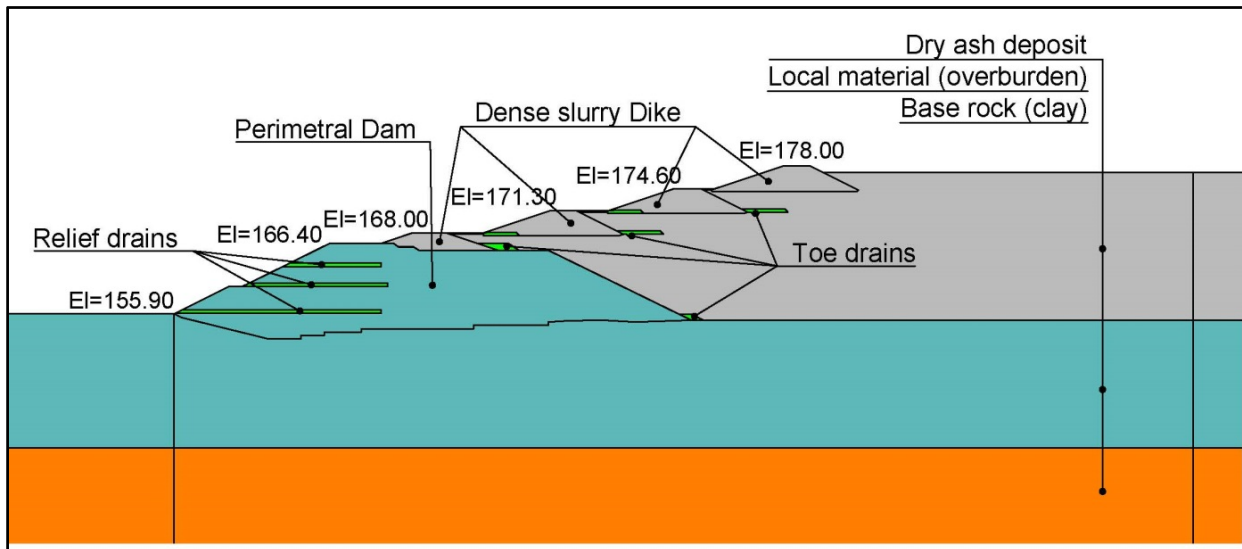


Fig. 3 - Ash Pond Analyzed Section A-A, Perimetral Dam and Dikes, 178.00 m a.s.l.

The stability of the impoundment was analyzed in a section that describes the current state, as presented in Fig. 3, and the case in which in the same section, the impoundment reaches its maximum designed height of 35.30 m at 191.30 m a.s.l. (see Fig. 4), considering no other interventions in material properties, methods of deposit management and no other modifications regarding the current equipment.

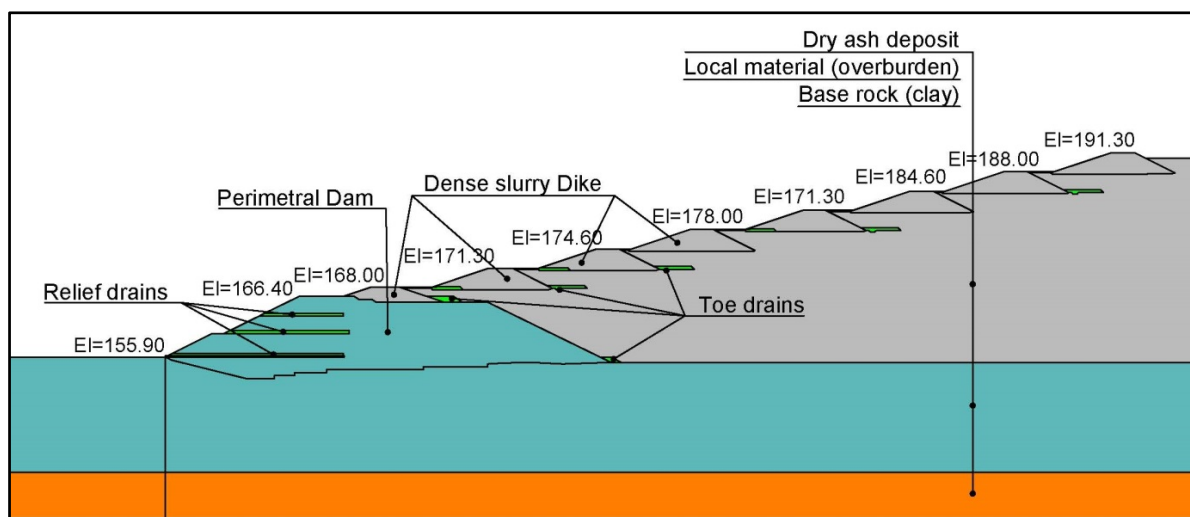


Fig. 4 - Ash Pond Analyzed Section A-A, Perimetral Dam and Dikes, 191.30 m a.s.l.

### 3.2 Materials used in model

The Gârla impoundment is constructed on a thick bed of overburden deposited on the previous coal excavation site. This overburden is mainly composed of clayey sand, sand, gravel and rock from the base rock that was exposed by the excavation process. Various layers of materials are present on site of the impoundment, with thickness varying from 20 m to 55 m from the S to the N of the deposit.

Laboratory studies returned the following characteristics (see Table 1) for the various materials identified on site:

Table 1

Geotechnical parameters of materials from laboratory tests

Material	Unit weight $\gamma$ [ kN/m <sup>3</sup> ]	Angle of internal friction $\phi$ [ ° ]	Cohesion $c$ [ kPa ]
Clay	17.30 – 19.30	6 – 13	18 – 27
Clayey Loam	17.10 – 17.60	3 – 6	16 – 20
Sandy Clay	18.50	14	10
Clayey Sand	17.90 – 19.60	15 – 18	2 – 3
Dry slurry	13.90	30	5
Overburden*	19.50	20	15

\* used in Perimetral Dam

Permeability coefficients ( $k$ ) of the materials found on site confirms the heterogeneous character of the overburden, ranging from  $5.0 \times 10^{-5}$  m/s and  $5.0 \times 10^{-11}$  m/s.

### 3.3 Finite element model and stability analysis

The program used in the stability analysis of the deposit is GeoStudio v7.23, modules SEEP/W and SLOPE/W, creating a coupled bidimensional analysis.

The extended dimensions of the model considered are (see Fig. 5 and Fig. 6):

- Section at El = 178.00 m a.s.l. : 375.00 x 74.80 m
- Section at El = 191.30 m a.s.l. : 375.00 x 88.00 m

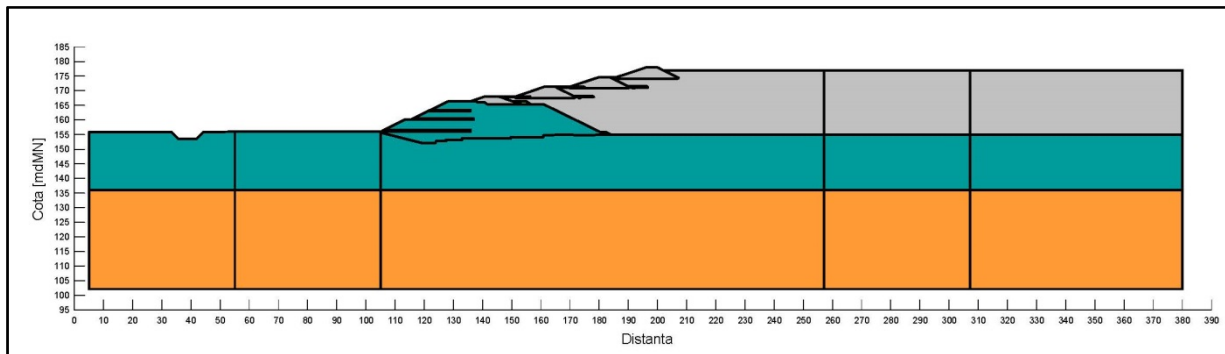


**Fig. 5** - Section A-A, Model dimensions, 178.00 m a.s.l.

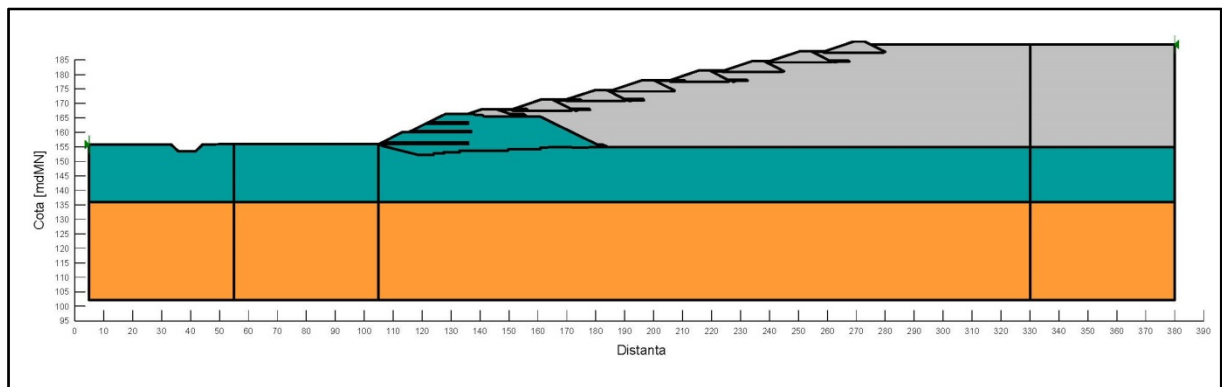


**Fig. 6** - Section A-A, Model dimensions, 191.30 m a.s.l.

The extended dimensions of the model were determined on one hand from general modeling criteria,

- Width of model = 1.50 – 3.0 x Height of modeled object
- Height of model = 2.00 – 3.00 x Height of modeled object,

and then manually adjusting the model dimensions in respect with the results (e.g. slip surface is not contained in model).

The model was discretized in finite elements composed of compatible Quadrilaterals and Triangles. The finite element size is variable ranging from 4.00 m on the edges of the model and gradually reducing its size to 1.00 m in the regions that make up the perimetral dam and the dense slurry dikes. The size of the elements decreases in increments of 0.50 to assure node compatibility.

An example of the distribution of finite elements is shown only for Section A-A at 191.30 m a.s.l. in Fig. 7, discretization of the model in Section A-A at 178.00 m a.s.l. was made similar.

The discretization is needed only in the seepage analysis, the resulting pore water pressure distribution, hence total head is then used as input for the stability analysis using SLOPE/W.

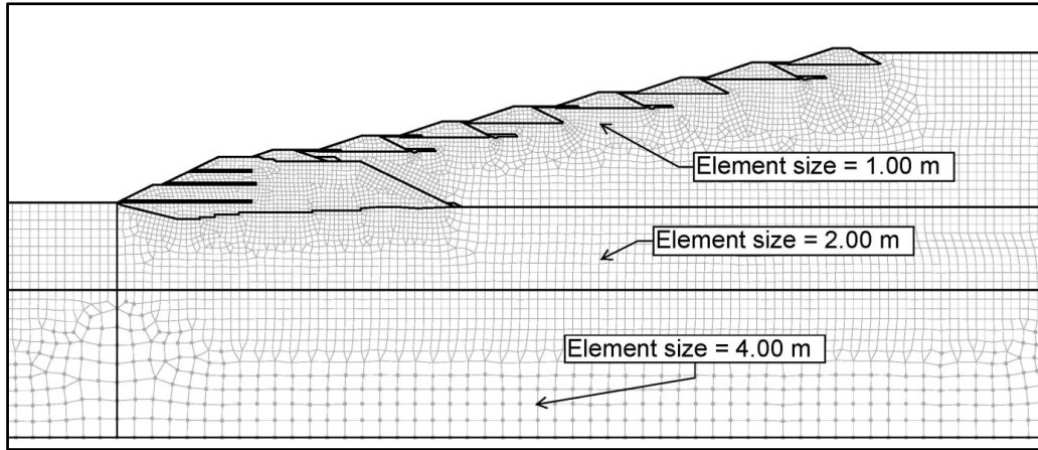


Fig. 7- Section A-A, Model discretization, 191.30 m a.s.l.

Using SEEP/W, based on material properties presented in Table 2, the position of the piezometric line or water table was determined for each analyzed hypothesis presented in Table 4.

The material properties used in the seepage and stability analysis are presented next:

Table 2

Geotechnical parameters of materials used in analysis

Material	Unit weight $\gamma$ [ kN/m <sup>3</sup> ]	Angle of internal friction $\phi$ [ ° ]	Cohesion $c$ [ kPa ]	Permeability coefficients (saturated) [ m/s ]
Overburden*	19.50	20	15	$5.50 \times 10^{-6}$
Dry slurry	13.90	30	5	$1.00 \times 10^{-5}$
Clay	19.50	20	15	$1.00 \times 10^{-9}$
Granular material**	20	34	0	$1.00 \times 10^{-3}$

\* used in Perimetral Dam

\*\* used in toe drains

The seepage analysis in SEEP/W is bidimensional, the material permeability is considered as a saturated model only, with constant conductivity in every direction under steady-state conditions.

The equation that describes the flow in this case can be expressed as:

$$\frac{\partial}{\partial x} \left( k_x \frac{\partial H}{\partial x} \right) + \frac{\partial}{\partial y} \left( k_y \frac{\partial H}{\partial y} \right) + Q = 0 \quad (1)[8]$$

$H$  – the total head

$k_x, k_y$  – the hydraulic conductivity in the x and y -direction

$Q$  – the applied boundary flux

The right side of equation (1) is null in this case because the material is considered to have a uniform and constant permeability, the full form of the equation regarding variation of permeability is:

$$\frac{\partial}{\partial x} \left( k_x \frac{\partial H}{\partial x} \right) + \frac{\partial}{\partial y} \left( k_y \frac{\partial H}{\partial y} \right) + Q = m_w \gamma_w \frac{\partial H}{\partial t} \quad (2)[8]$$

$m_w$  – the slope of the storage curve

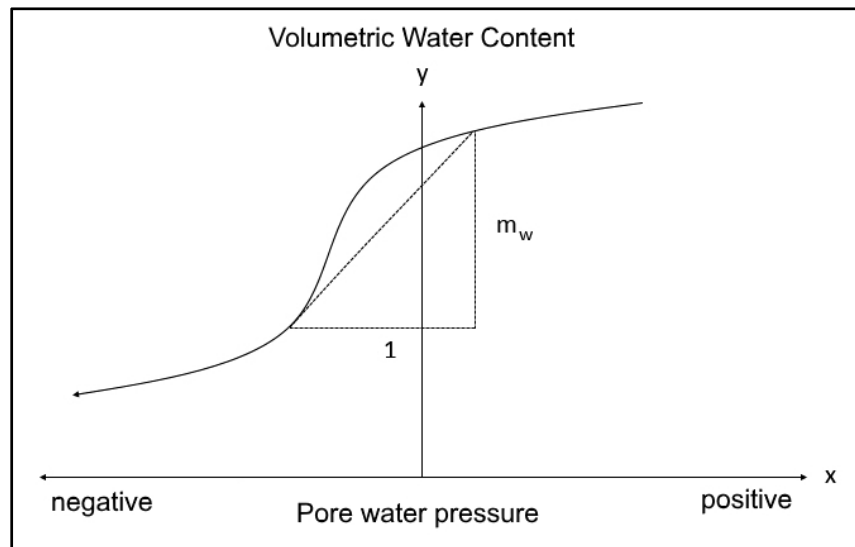


**Fig. 8-** Volumetric Water Content Variation

The permeability of the materials modeled is considered constant, the slope ( $m_w$ ) presented in Fig. 8 is null, in other words, the permeability does not change with respect to the variation of pore water pressure. We can assume a constant permeability given the fact that the seepage analysis is a steady-state analysis, the piezometric line can have slightly different positions in a transient analysis in which case the volumetric water content and the hydraulic conductivity function of the material must be known.

The stability analysis modeled in SLOPE/W is based on the GLE (General Limit Equilibrium) method that solves two Factor of Safety equations, one regarding forces and one regarding moments acting on the volume of material collapsing and sliding. The GLE method is based on the slice method first developed by Fellenius (1936) that was later enhanced by others (Janbu, Bishop, Morgenstern and Price et. al.).

Equations solved by SLOPE/W are applied to all the slices that divide the slip surface.

The forces that act on the sliding mass are presented in Fig. 9, these forces are used in the determination of the Factor of Safety using equations (3) and (4).

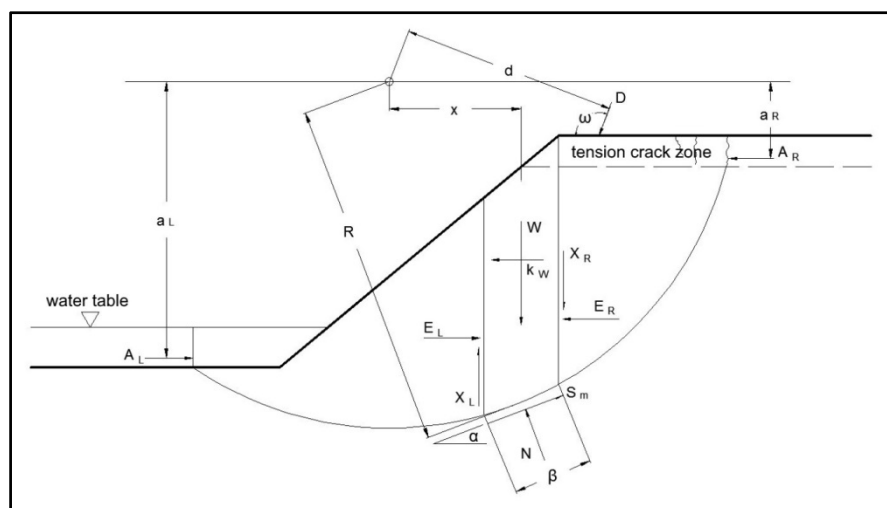


**Fig. 9 -** Forces acting on the sliding mass

- $W$  – the total weight of a slice of width  $b$  and height  $h$
- $N$  – the total normal force on the base of the slice
- $S_m$  – the shear force mobilized on the base of each slice.

- $E$  – the horizontal interslice normal forces. Subscripts L and R designate the left and right sides of the slice, respectively.
- $X$  – the vertical interslice shear forces. Subscripts L and R define the left and right sides of the slice, respectively.
- $D$  – an external point load.
- $kW$  – the horizontal seismic load applied through the centroid of each slice.
- $R$  – the radius for a circular slip surface or the moment arm associated with the mobilized shear force,  $S_m$  for any shape of slip surface.
- $f$  – the perpendicular offset of the normal force from the center of rotation or from the center of moments.
- $X$  – the horizontal distance from the centerline of each slice to the center of rotation or to the center of moments.
- $e$  – the vertical distance from the centroid of each slice to the center of rotation or to the center of moments.
- $d$  – the perpendicular distance from a point load to the center of rotation or to the center of moments.
- $H$  – the vertical distance from the center of the base of each slice to the uppermost line in the geometry (i.e., generally ground surface).
- $a$  – the perpendicular distance from the resultant external water force to the center of rotation or to the center of moments.
- $A$  – the resultant external water forces.
- $\Omega$  – the angle of the point load from the horizontal. This angle is measured counter-clockwise from the positive x-axis.
- $\alpha$  – the angle between the tangent to the center of the base of each slice and the horizontal.<sup>1</sup>

The formulated equation to determine the Factor of Safety regarding moments is:

$$FS_m = \frac{\sum(c'\beta R + (N-u\beta)R \tan \phi')}{\sum W_X - \sum Nf + \sum k_W e \pm \sum Dd \pm \sum Aa} \quad (3)[9]$$

- $c'$  – the effective cohesive strength of the material
- $\beta$  – the base length of each slice
- $u$  – the pore water pressure
- $\phi'$  – the effective frictional strength of the material

while the equation that determines the Factor of Safety with respect to forces is:

$$FS_f = \frac{\sum(c'\beta \cos \alpha + (N-u\beta) \tan \phi' \cos \alpha)}{\sum N \sin \alpha + \sum k_W - \sum D \cos \omega \pm \sum A} \quad (4)[9]$$

Based on the model presented and the materials considered, a number of 360 Factors of Safety were obtained using the modeling software, considering a number of 9 general hypotheses that are described in Table 4.

Each hypothesis is divided into two scenarios, a static and pseudo static analysis and each scenario returns two Factors of Safety (FoS), one FoS for a circular slip surface, and one for an optimized slip. These Factors of Safety are calculated for comparison purposes using 5 methods:

- Fellenius
- Bishop
- Janbu

<sup>1</sup> [9] GEO-SLOPE International Ltd. (February 2010). Stability Modeling with SLOPE/W 2007 Version an Engineering Methodology, Fourth Edition.

- Morgenstern – Price
- G.L.E.

The pseudo static method is used in analysis to simulate the effect of an earthquake by applying a force equal to the inertial forces that develop during the earthquake. The forces are computed by inserting a coefficient “k” that represents a percentage of the gravitational acceleration  $g = 9.807 \text{ m/s}^2$ .

The differences between the methods used in calculating the FoS are presented in Table 3 regarding the conditions of static equilibrium satisfied by each method.

Table 3[9]

**Conditions of static equilibrium satisfied by various limit equilibrium methods**

Method	Force Equilibrium		Moment Equilibrium
	1st Direction (e.g., Vertical)	2nd Direction (e.g., Horizontal)	
Fellenius	Yes	No	Yes
Bishop	Yes	No	Yes
Janbu	Yes	Yes	No
Morgenstern-Price	Yes	Yes	Yes*
G.L.E.	Yes	Yes	Yes

\* Moment equilibrium on individual slice is used to calculate interslice shear forces

The hypotheses analyzed are valid for both the seepage model and the stability model, boundary conditions are used to simulate different scenarios of water table and drainage capacity as described in Table 4.

Table 4

**Hypotheses analyzed**

Hypotheses analyzed	Description of hypothesis
0	Dense Slurry Pipelines operational, no phreatic horizon, toe drain 100% drainage capacity
1	Dense Slurry Pipelines operational, phreatic horizon at 18 m depth, toe drain 100% drainage capacity
2	Dense Slurry Pipelines non-operational, phreatic horizon at 18 m depth
3	Dense Slurry Pipelines operational, phreatic horizon at 18 m depth, toe drain 50% drainage capacity
4	Dense Slurry Pipelines operational, phreatic horizon at 18 m depth, toe drain 25% drainage capacity
5	Dense Slurry Pipelines operational, phreatic horizon at 18 m depth, toe drain 5% drainage capacity
6	Dense Slurry Pipelines operational, phreatic horizon at 18 m depth, toe drain 0% drainage capacity (fully clogged)
7	Dense Slurry Pipelines operational, phreatic horizon at 10 m depth, toe drain 100% drainage capacity
8	Dense Slurry Pipelines operational, phreatic horizon at 10 m depth, toe drain 0% drainage capacity

Regarding the hypotheses used in the model, hypothesis 0 represents the best simulation of reality given the fact that no phreatic horizon is observed in none of the geotechnical studies.

In extreme conditions of seepage during heavy rain we can assume that a water table can develop outside the impoundment and this can be combined with the hypothesis that toe drains can suffer clogging over an extensive period of drainage and no maintenance.

All these extreme conditions can then be superimposed with an earthquake to simulate a non-realistic scenario, but still these scenarios were modeled to better understand the behavior of such a complex structure.

#### 4. Results and remarks

Given the fact that the number of hypotheses analyzed is very large, only a significant number of diagrams will be presented next, all the results are presented in tabular form.

The FoS presented in the diagrams corresponds to the G.L.E. method, with a optimized slip surface.

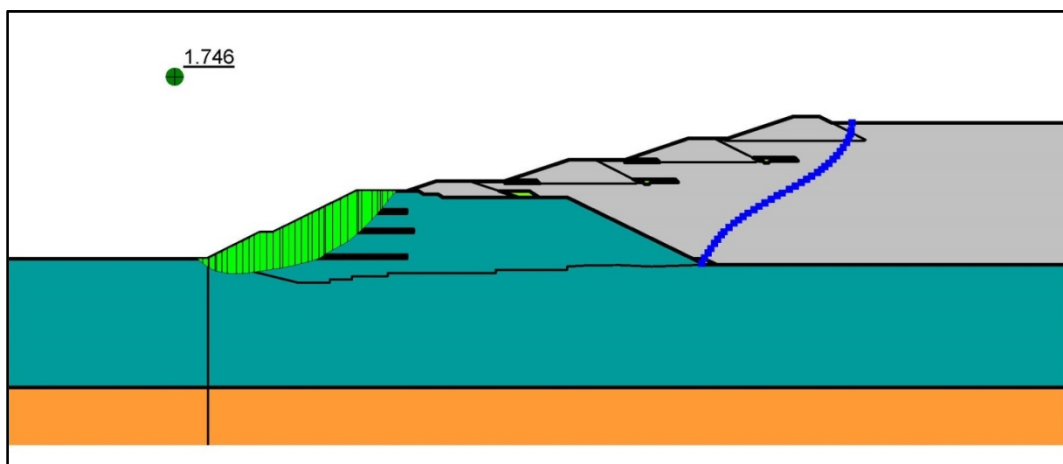


**Fig. 10** - Section A-A, FoS, Hypothesis 0, Static, 178.00 m a.s.l.

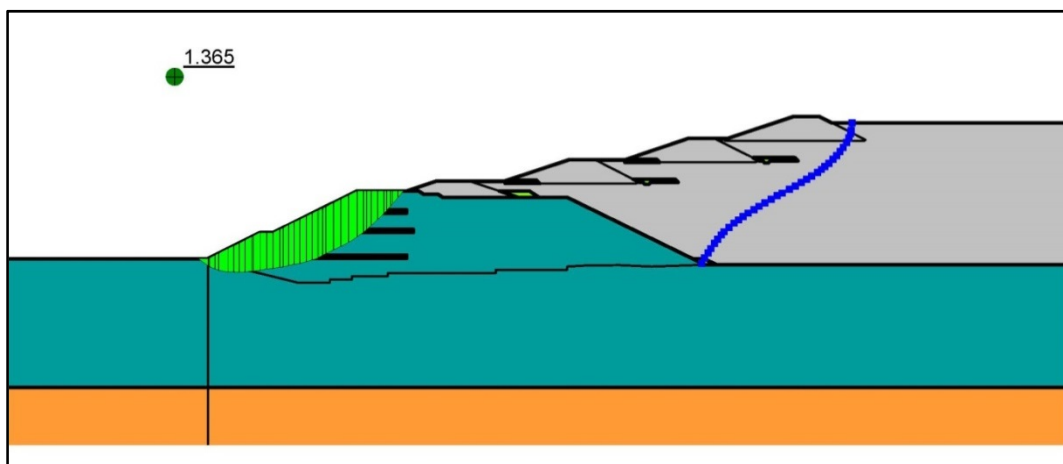


**Fig. 11** - Section A-A, FoS, Hypothesis 0, Pseudo Static ( $kh=0.1g$ ), 178.00 m a.s.l.

The first and most realistic hypothesis results in a FoS of 1.746 for the static analysis and 1.365 for the pseudo static one using a horizontal coefficient of 0.1, both results are satisfactory regarding the stability of the structure considering that an FoS of 1 is acceptable, during an earthquake the FoS of such a structure can have values below 1.00 for short amounts of time but not long enough to activate any sliding masses.

The overall stability of the perimetral dam is not influenced very much by the pseudo static analysis because the piezometric line is not crossing the slip surface, thus, only the inertial forces are added to the destabilizing effect.

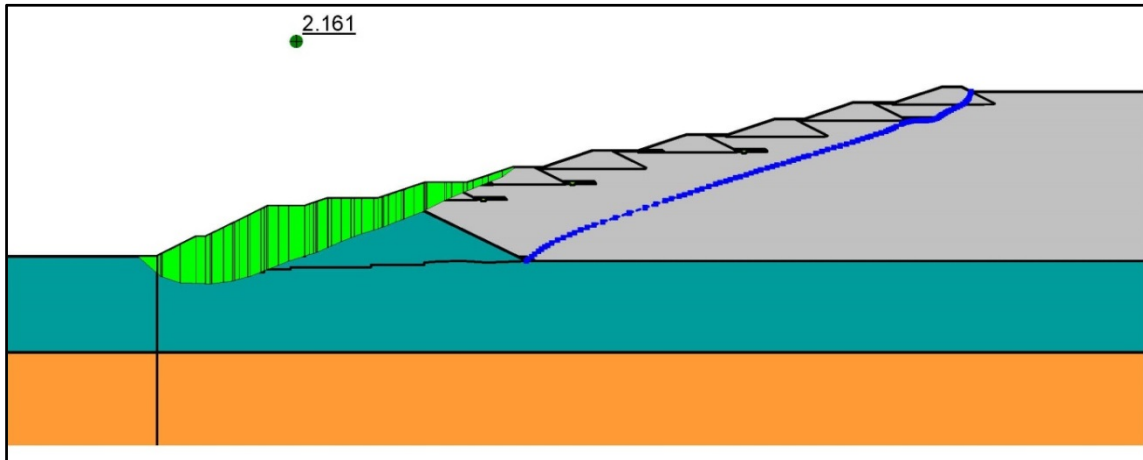


**Fig. 12** - Section A-A, FoS, Hypothesis 0, Static, 191.30 m a.s.l.

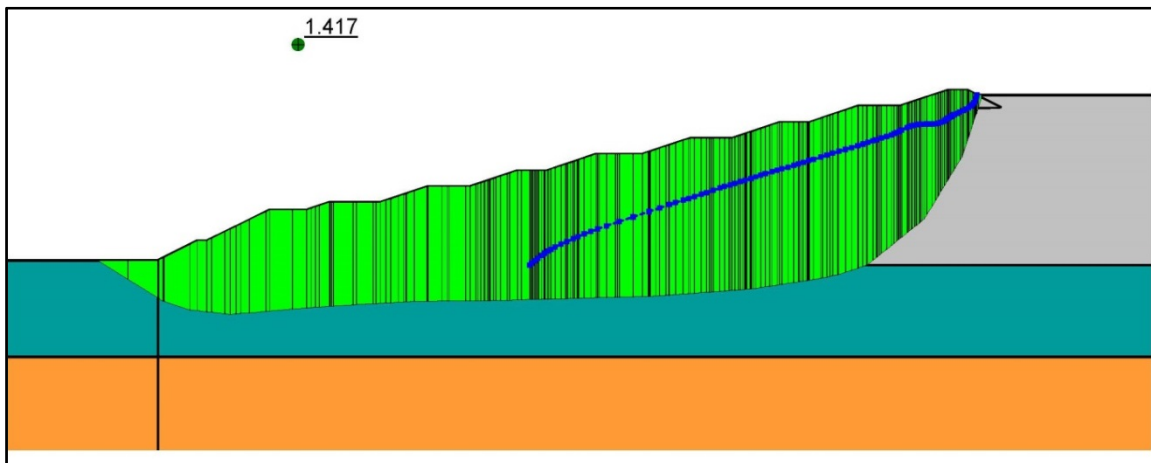


**Fig. 13** - Section A-A, FoS, Hypothesis 0, Pseudo Static ( $kh=0.1g$ ), 191.30 m a.s.l.

In the scenario at 191.30 m a.s.l. the FoS is higher than at 178.00 m a.s.l.. One explanation for this behavior may be related to the fact that the resisting forces acting on the base of the sliding mass are much higher with respect to the total weight of the sliding mass than in the case at 178.00 m a.s.l..

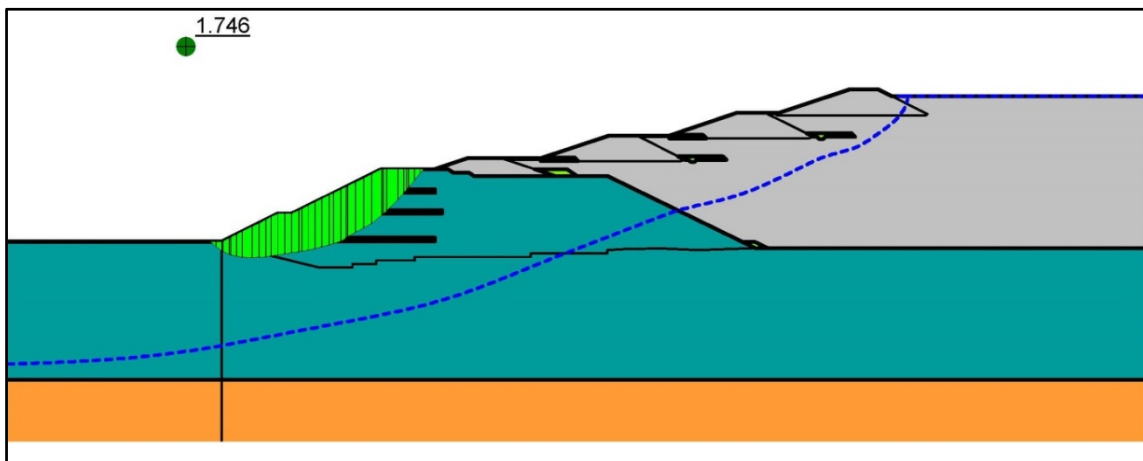


**Fig. 14** - Section A-A, FoS, Hypothesis 3, Static, 178.00 m a.s.l.

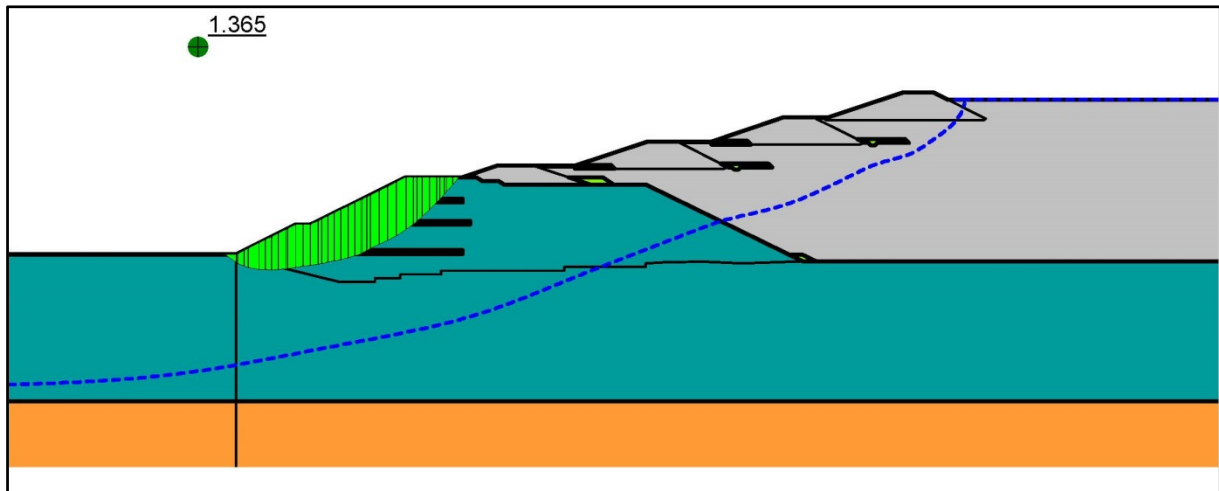


**Fig. 15** - Section A-A, FoS, Hypothesis 3, Pseudo Static ( $kh=0.1g$ ), 178.00 m a.s.l.

In hypothesis 3 the FoS does not change for the scenario at 178.00 m a.s.l. because, again the piezometric line does not come into contact with the sliding mass.

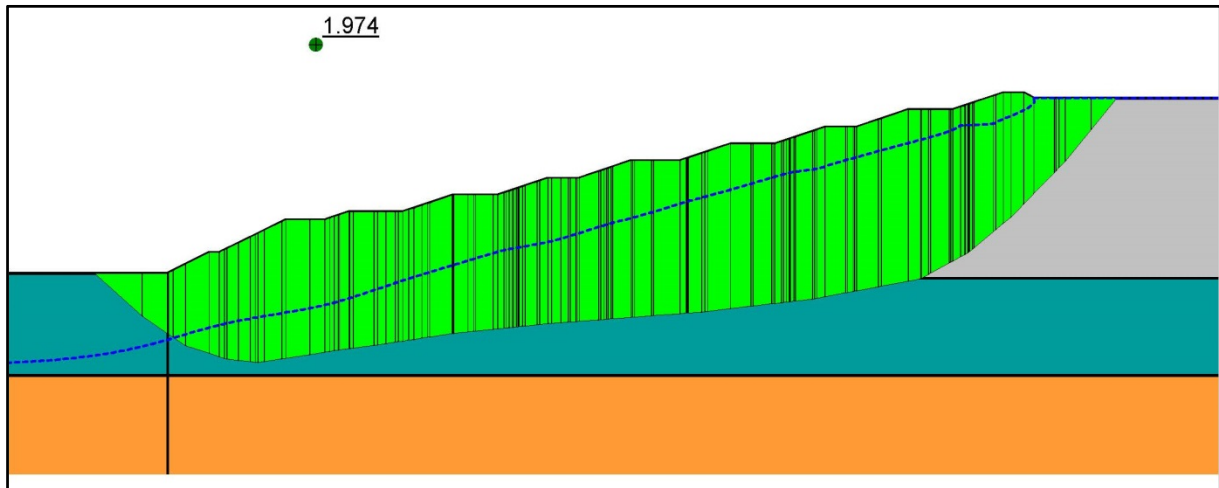


**Fig. 16** - Section A-A, FoS, Hypothesis 3, Static, 191.30 m a.s.l.

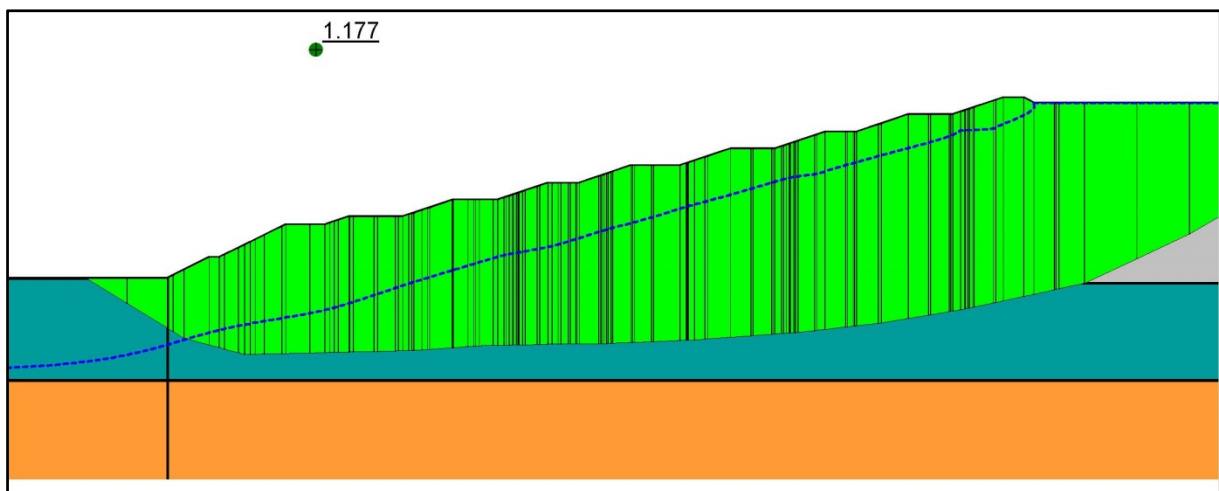


**Fig. 17** - Section A-A, FoS, Hypothesis 3, Pseudo Static ( $kh=0.1g$ ), 191.30 m a.s.l.

The FoS is significantly reduced in hypothesis 3, when the structure is at 191.30 m a.s.l., 1.974 in static and 1.177 in the pseudo static case. Although the slip surface presents a very large area the factor of safety is still well in acceptable limits.

The rest of the results are presented tabular:

Table 5

Factors of Safety, 178.00 m a.s.l. scenario

Static / Pseudostatic analysis (kh = 0.1g), (178.00 maSL)							
Hypothesis analyzed		Method of analysis					
		Factor of Safety					
No.	Slip surface type (shape)	Fellenius	Bishop	Janbu	Morgenstern Price	G.L.E.	
0	0.1	I	1.640	1.892	1.604	1.743	1.746
		II	1.754	1.862	1.739	1.857	1.857
	0.2	I	1.332	1.519	1.264	1.370	1.365
		II	1.341	1.430	1.322	1.426	1.426
1	1.1	I	1.640	1.892	1.604	1.743	1.746
		II	1.754	1.862	1.739	1.857	1.857
	1.2	I	1.333	1.518	1.261	1.370	1.365
		II	1.341	1.430	1.322	1.426	1.426
2	2.1	I	1.640	1.892	1.604	1.743	1.746
		II	1.754	1.862	1.739	1.857	1.857
	2.2	I	1.333	1.518	1.261	1.370	1.365
		II	1.341	1.430	1.322	1.426	1.426
3	3.1	I	1.640	1.892	1.604	1.743	1.746
		II	1.754	1.862	1.739	1.857	1.857
	3.2	I	1.333	1.518	1.261	1.370	1.365
		II	1.341	1.430	1.322	1.426	1.426
4	4.1	I	1.640	1.892	1.604	1.743	1.746
		II	1.754	1.862	1.739	1.857	1.857
	4.2	I	1.333	1.518	1.261	1.370	1.365
		II	1.341	1.430	1.322	1.426	1.426
5	5.1	I	1.640	1.892	1.604	1.743	1.746
		II	1.754	1.862	1.739	1.857	1.857
	5.2	I	1.333	1.518	1.261	1.370	1.365
		II	1.341	1.430	1.322	1.426	1.426
6	6.1	I	1.640	1.892	1.604	1.743	1.746
		II	1.754	1.862	1.739	1.857	1.857
	6.2	I	1.333	1.518	1.261	1.370	1.365
		II	1.341	1.430	1.322	1.426	1.426
7	7.1	I	1.640	1.892	1.604	1.743	1.746
		II	1.754	1.862	1.739	1.857	1.857
	7.2	I	1.333	1.518	1.261	1.370	1.365
		II	1.341	1.430	1.322	1.426	1.426
8	8.1	I	1.640	1.892	1.604	1.743	1.746
		II	1.754	1.862	1.739	1.857	1.857
	8.2	I	1.574	1.701	1.242	1.310	1.308
		II	1.222	1.383	1.281	1.380	1.381

Factors of Safety, 191.30 m a.s.l. scenario

Static / Pseudostatic analysis (kh = 0.1g), (191.30 maSL)							
Hypothesis analyzed		Method of analysis					
		Factor of Safety					
No.	Slip surface type (shape)	Fellenius	Bishop	Janbu	Morgenstern Price	G.L.E.	
0	0.1	I	2.395	2.293	2.083	2.161	2.161
		II	2.522	2.586	2.520	2.582	2.582
	0.2	I	1.211	1.793	1.480	1.417	1.417
		II	1.425	1.584	1.465	1.573	1.573
1	1.1	I	1.809	2.688	2.020	2.142	2.150
		II	2.042	2.313	2.142	2.303	2.304
	1.2	I	1.284	1.697	1.207	1.253	1.246
		II	1.191	1.300	1.239	1.292	1.292
2	2.1	I	2.395	2.293	2.083	2.183	2.164
		II	2.522	2.586	2.519	2.582	2.582
	2.2	I	1.675	1.701	1.473	1.576	1.539
		II	1.659	1.702	1.649	1.698	1.698
3	3.1	I	1.660	2.474	1.876	1.974	1.974
		II	1.916	2.167	2.009	2.155	2.156
	3.2	I	1.159	1.576	1.131	1.177	1.177
		II	1.110	1.219	1.163	1.212	1.212
4	4.1	I	1.385	2.380	1.756	1.926	1.944
		II	1.607	2.044	1.834	2.018	2.021
	4.2	I	1.060	1.502	1.087	1.129	1.126
		II	1.062	1.175	1.119	1.166	1.167
5	5.1	I	1.271	2.225	1.642	1.813	1.833
		II	1.492	1.926	1.731	1.902	1.904
	5.2	I	0.952	1.446	1.018	1.090	1.090
		II	0.923	1.130	1.043	1.120	1.120
6	6.1	I	1.226	2.170	1.604	1.768	1.786
		II	1.463	1.897	1.705	1.873	1.875
	6.2	I	0.888	1.416	0.999	1.074	1.073
		II	0.909	1.114	1.029	1.105	1.105
7	7.1	I	1.736	2.594	1.951	2.069	2.081
		II	1.982	2.250	2.084	2.241	2.241
	7.2	I	1.234	1.637	1.174	1.222	1.215
		II	1.164	1.272	1.213	1.264	1.264
8	8.1	I	1.165	2.104	1.553	1.715	1.727
		II	1.409	1.842	1.656	1.818	1.821
	8.2	I	0.852	1.374	0.970	1.044	1.045
		II	0.883	1.087	1.004	1.077	1.078

Note:

*I, II represents the shape of the slip surface, I – optimized, II – circular  
X.1 and X.2 represents the type of analysis, X.1 – static, X.2 – pseudo static, where X is the number of the hypotheses analyzed from 0 to 8.*

## 5. Conclusions

The overall stability of the Gârla impoundment serving the Rovinari coal-fired power plant was analyzed in a number of 9 general hypotheses based on the existing and known insitu conditions.

The hypotheses were extended furthermore by simulating the effect of an earthquake by using a pseudo static approach and comparing results for different methods as presented in Table 3.

A number of 8 diagrams are presented, regarding hypothesis 0 and 3, which are considered the most realistic.

The analysis revealed the fact that considering the material properties presented in Table 2 and the hypotheses presented in Table 4, the overall FoS (Factor of Safety) of the impoundment is considered acceptable, above 1.0 in general.

The model and hypotheses analyzed are based on theoretical modelled characteristics of the materials used in the Gârla impoundment. The current state of the impoundment is stable and can be considered stable in the future based on the presented results. A more comprehensive study with more accurate modelled material properties can be used in the future to better reflect the overall stability.

## References

- [1] Stematiu D. (1988). *Calculul Structurilor Hidrotehnice prin Metoda Elementelor Finite* (in Romanian), București, Editura Tehnică.
- [2] Prișcu R. (1974). *Construcții Hidrotehnice*, Volumul II, București, Editura Didactică și Pedagogică (in Romanian).
- [3] Shreya N., Biswajit P. (2012). *Compaction and Hydraulic Conductivity Analysis of Fly ash of B.T.P.S. for the construction of a Natural Geoliner*.
- [4] Dewberry Consultants LLC Fairfax, Virginia, (2013). Coal Combustion Residue Impoundment Round 11 - Dam Assessment Report Cumberland Fossil Plant Dry Ash Storage / Ash Pond TVA Cumberland City, Tennessee.
- [5] Shivakumar S. et. al. (2015). Seepage and Stability Analyses of Earth Dam Using Finite Element Method, International conference on water resources, coastal and ocean engineering (ICWRCOE 2015), Aquatic Procedia 4, pp. (876 – 883).
- [6] Zhou De-quan et. al. (2008). *Geological behavior of wet outflow deposition fly ash*, DOI: 10.1007/s11771-008-0436-6.
- [7] Muntean M.D., Morariu A. (2014). The influence of slag and ash deposit used by Drobeta -Turnu Severin power plant concerning groundwater in the area, Journal of Young Scientist, Volume II, ISSN Online 2344 - 1305.
- [8] GEO-SLOPE International Ltd. (February 2010). Seepage Modeling with SEEP/W 2007 an Engineering Methodology, Fourth Edition.
- [9] GEO-SLOPE International Ltd. (February 2010). Stability Modeling with SLOPE/W 2007 Version an Engineering Methodology, Fourth Edition.